

SYNTHESIS AND COMPARATIVE STUDY OF THE INHIBITIVE PROPERTIES OF ISOMERIC SCHIFF BASES AND ITS CYCLISATION PRODUCTS

N.Thamaraiselvi, K. Parameswari, S. Chitra,

Department of Chemistry, PSGR Krishnammal College for Women,
Coimbatore, Tamilnadu, India

A.Selvaraj*

C.B.M. College, Coimbatore, Tamilnadu, India

Abstract

The corrosion behaviour of mild steel in 1M sulphuric acid solution and its inhibition by Schiff bases and thiazolidinones was studied using weight loss method at various temperatures (303-333K), by electrochemical and non – electrochemical techniques. The percentage inhibition efficiency of the inhibitors increased with increase in inhibitor concentration. Potentiodynamic polarization studies revealed that though the Schiff bases and thiazolidinones act as mixed type inhibitors they are slightly anodic in nature. Adsorption of these inhibitors on the mild steel surface followed the Langmuir adsorption isotherm. The thermodynamic parameters such as activation energy (E_a) and free energy of adsorption (ΔG°_{ads}) were calculated. The synergistic effect of halide ions on the inhibition efficiency of thiazolidinones was also studied.

Key words

Corrosion inhibition, mild steel, Schiff bases, thiazolidinones, inhibition efficiency, Langmuir adsorption

Introduction

Acid solutions are widely used in industry, the most important fields of application being acid pickling, industrial acid cleaning, acid descaling and oil well acidising. Due to the general aggressivity of acid solutions the practice of inhibitor is commonly used to reduce the corrosive attack on metallic materials. Inhibitors are generally used in this process to control the metal dissolution as well acid consumption. In general, organic compounds such as amines, heterocyclic compounds, acetylinic alcohol have been used as inhibitors in industrial applications¹⁻⁵.

* Author for correspondence

Mild steel specimens (composition: C-0.084, Mn-0.369, Si-0.129, P-0.025, S-0.027, Cr-0.022, Mo-0.011, Ni-0.013, Iron-rest %) of size 5 cm × 2 cm × 0.05cm were used for weight loss and gasometric measurements. For electrochemical methods, mild steel rods of same composition with an exposed area of 0.785 cm² was used. The electrode was polished using 1/0, 2/0, 3/0 and 4/0 grades of emery sheets and degreased with trichloro ethylene. All the chemicals used for the synthesis of the inhibitors were of analar grade.

Synthesis of inhibitors

Ortho/meta/para – amino phenol (0.1M) was dissolved in alcohol and (0.1M) benzaldehyde was added to it. This mixture was refluxed for an hour. The Schiff bases (1-3) obtained on cooling was filtered and recrystallised. The Schiff base was dissolved in DMF and 15 ml of thioglycolic acid was added, refluxed with stirring for about 6 hours. The thiazolidinones (4-6) was washed with 10 % NaHCO₃ solution. Filtered, dried and recrystallised from dioxane. Structure of the synthesised compounds (1-6) are given in table 1.

Non Electrochemical methods

Weight loss method

Weight loss experiments were carried out by immersing preweighed mild steel specimens in 200 ml of inhibited and uninhibited solutions in triplicates. After a period of 3 hours the specimens were removed, washed, dried and weighed. From the initial and final masses of the specimen, the loss in weight was calculated. The experiment was repeated for various inhibitor concentrations in 1M H₂SO₄.

From the loss in weight, corrosion rate, inhibition efficiency, surface coverage (θ) were calculated using the formula.

$$\text{Efficiency of inhibitor} = \frac{(\text{Weight loss without inhibitor} - \text{Weight loss with inhibitor})}{\text{Weight loss without inhibitor}} \times 100$$

$$\text{Corrosion rate (mpy)} = \frac{534 \times \text{Weight loss in mgms}}{\text{Density} \times \text{area in sq. inch} \times \text{Time in hours}}$$

$$\text{Surface coverage}(\theta) = \frac{(\text{Weight loss without inhibitor} - \text{Weight loss with inhibitor})}{\text{Weight loss without inhibitor}}$$

To know the effect of temperature the weight loss method was carried out at different temperature ranges (ie.) 40°C-60°C using a thermostat. From the weight loss, inhibition efficiency, corrosion rate, activation energy (E_a) and free energy of adsorption ($\Delta G^\circ_{\text{ads}}$) were calculated. Activation energy was calculated by graphical method by plotting log corrosion rate vs $1000/T(K)$ for temperature range of 30-60°C in 1M H_2SO_4 with and without inhibitor at a concentration of 10 mM.

$$E_a = 2.303 \times 8.314 \times \text{slope } J$$

$$\Delta G^\circ_{\text{ads}} = -RT \ln (55.5K)$$

The above equations were used to calculate activation energy and free energy of adsorption.

Gasometric method

Polished and degreased mild steel specimens were suspended from the hook of the glass stopper and were introduced into the cell containing 200 ml of 1M H_2SO_4 . The same procedure was repeated with 1M H_2SO_4 containing various concentrations of inhibitors. From the volume of hydrogen gas liberated, the inhibition efficiency was calculated using the formula.

$$\text{Inhibition efficiency (\%)} = \frac{V_B - V_I}{V_B} \times 100$$

Where,

V_B is the volume of H_2 evolved in the absence of inhibitors

V_I is the volume of H_2 evolved in the presence of inhibitor.

Electrochemical studies

Potentiodynamic polarization and impedance measurements

Electrochemical studies were carried out for mild steel rod of same composition both in the presence and absence of inhibitors using a potentiostat (model 1280 B solartron, UK). The electrochemical investigations were carried out in a three electrode cell assembly with platinum electrode as the counter electrode, a saturated calomel electrode as the reference electrode and the mild steel electrode as the working electrode. The EIS measurements were made at corrosion potential over a frequency range of 10 kHz to 0.01 Hz with a signal amplitude of 10 mV. From these

studies the charge transfer resistance (R_t), double layer capacitance (C_{dl}) and inhibition efficiency were calculated.

$$\text{Inhibition efficiency (\%)} = \frac{R_{t(\text{inh})} - R_{t(\text{blank})}}{R_{t(\text{inh})}} \times 100$$

Where,

$R_{t(\text{inh})}$ is the charge transfer resistance in the presence of inhibitor

$R_{t(\text{blank})}$ is the charge transfer resistance in the absence of inhibitor

After EIS measurements the polarization measurements were carried out at a potential range of -200 mV to +200 mV with respect to open circuit potential at a scan rate of 1 mV/sec.

$$\text{Inhibition efficiency (\%)} = \frac{I_{\text{corr}(\text{blank})} - I_{\text{corr}(\text{inh})}}{I_{\text{corr}(\text{blank})}} \times 100$$

Where,

$I_{\text{corr}(\text{blank})}$ is the corrosion current in the absence of inhibitor

$I_{\text{corr}(\text{inh})}$ is the corrosion current in the presence of inhibitor.

Synergistic effect

The synergistic effect was studied by the addition of 1mM KI to the steel specimen immersed in 1M H_2SO_4 containing various concentrations of the thiazolidinones for a duration of 3 hours. From the weight loss data, the corrosion rate and inhibition efficiency were calculated. The same procedure was repeated by the addition of 1mM KCl and 1 mM KBr.

Atomic absorption spectroscopic studies

Atomic absorption spectrophotometer (model GBC 908, Australia) was used for estimating the amount of dissolved iron in the corroded solution containing various concentrations of thiazolidinones in 1M H_2SO_4 after exposing the mild steel specimen for three hours. From the amount of dissolved iron, the inhibition efficiency was calculated.

$$\text{Percentage inhibition efficiency} = \frac{B - A}{B} \times 100$$

Where,

A is the amount of dissolved iron in presence of inhibitor

B is the amount of dissolved iron in the absence of inhibitor

Weight loss data

Table 2 gives the value of inhibition efficiency obtained from weight loss measurements at $30 \pm 1^\circ\text{C}$ for different concentrations of Schiff bases and thiazolidinones. The weight loss data is depicted graphically by plotting inhibition efficiency vs inhibitor concentration (fig.1). It has been observed that the inhibition efficiency for all the inhibitors increased with increase in concentration of inhibitors. The weight loss data obtained at higher temperatures and the corresponding thermodynamic parameters are given in tables 3 & 4 respectively. The data reveals that inhibition efficiency decreases with increase in temperature.

Gasometry

Table 5 gives the values of inhibition efficiency obtained from gasometric method for mild steel in 1M H_2SO_4 and 1M H_2SO_4 containing selected concentrations of inhibitor. The volume of gas collected decreased with the addition of inhibitors and the data obtained was found to be good agreement with that obtained by weight loss method.

AC-impedance measurement

The electrochemical impedance measurements were carried out for mild steel in 1M H_2SO_4 in the absence and presence of selected concentrations of inhibitor. The impedance spectra are shown in fig. 4. The R_t , C_{dl} values and inhibition efficiency are presented in the table 6.

Potentiodynamic polarization

Polarization curves for mild steel in 1M H_2SO_4 for the inhibitors are shown in fig. 5. The values of corrosion current (I_{corr}), corrosion potential (E_{corr}), cathodic and anodic Tafel slopes (b_a & b_c), the inhibition efficiency calculated from I_{corr} are given in Table 7.

Discussion

The very high inhibition efficiency of the anils can be attributed to their structure. The inhibition of corrosion of mild steel by these compounds is mainly due to the formation of a stable film on the metal surface. The mechanism of adsorption

responsible for the corrosion inhibition for the set of aromatic Schiff bases employed in the present investigation can be explained as follows:– All the three Schiff bases contain two aromatic rings and one $-\text{CH}=\text{N}-$ group. Hence they are expected to have adsorbed on the metal surface through the combination of three adsorption mechanisms.

- (i) Electrostatic interaction between the charged molecule and the charged metal surface (fig.A).

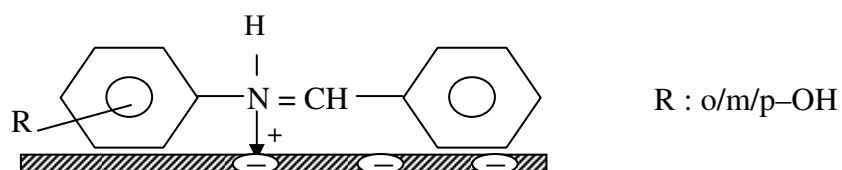


Fig. A

- (ii) Interaction of unshared electron pairs in the molecule and the charged metal surface (fig. B).

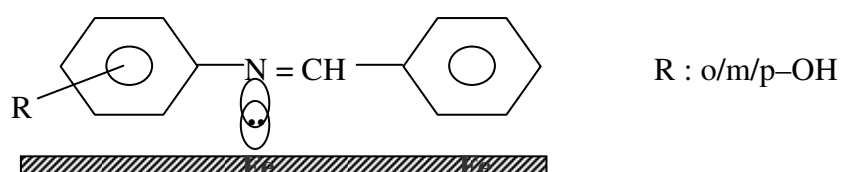


Fig. B

- (iii) Interaction of π -electrons of the aromatic ring and $-\text{CH}=\text{N}-$ group with the metal surface (fig.C).

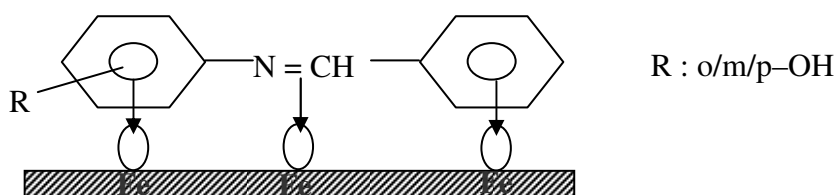


Fig. C

The above three interactions are facilitated by the flat orientation of the molecule with respect to the metal surface. All the three mechanisms might have contributed to the adsorption of the anils on the metal surface.

The order of inhibition efficiency of the anils are

OBAP > MBAP > PBAP

The ortho isomer has higher inhibition efficiency than the meta and para isomer. The difference in the extent of inhibition efficiency of the anils may be due to the tendency to form amine cation $-\text{N}^+\text{H}$ in acidic solution. This tendency is enhanced by the presence of ortho $-\text{OH}$ group which can readily interact with the negatively charged metal surface due to the ortho effect⁶⁻⁹. This leads to more adsorption of the ortho isomer followed by meta and para isomers in the decreasing order.

The inhibition efficiency of the thiazolidinones follows the order
TPAP>TOAP>TMAP

The inhibition efficiency of all the thiazolidinones was found to be excellent providing 96-99% inhibition. The inhibition efficiency of PBAP has been drastically increased from 78 % to 99.31 % (at 10 mM). Similarly for MBAP the percentage inhibition efficiency increased from 92-96%. OBAP has a very high inhibition efficiency of 99.28 % (10 mM). In general it can be concluded that the inhibition efficiency of all the 3 isomeric Schiff bases has been enhanced as a result of cyclisation. Cyclisation did not result in the formation of an aromatic ring. Hence the increased inhibition efficiency may not be due to the formation of the cyclic product. Therefore the best performance of the isomeric thiazolidinones may be attributed to the introduction of sulphur atom during cyclisation.

Adsorption isotherm

The degree of surface coverage (θ) for different concentrations of inhibitors in 1M H_2SO_4 was evaluated from weight loss data. Langmuir isotherm was tested by plotting C/θ vs C for the inhibitors. A straight line was obtained in all the cases proving the fact that the adsorption of these compounds on mild steel surface obeys Langmuir adsorption isotherm (fig.2).

Effect of temperature

The inhibition efficiency given in table 2 reveals that inhibition efficiency decreases with increase in temperature. The value of E_a in the inhibited acid solutions is greater than those obtained in the uninhibited acid solution (Table 3). This suggests that the corrosion of mild steel occurs at the uncovered part of the electrode surface and that adsorption occurs at high energy sites¹⁰. The less negative $\Delta G^\circ_{\text{ads}}$ (Table 4)

confirms the physical adsorption of the inhibitors on the metal surface. Arrhenius plots (log corrosion rate vs $1/T$) for mild steel in 1M H_2SO_4 at different concentration of inhibitors are given in fig.3.

Electrochemical studies

The AC impedance diagrams for solutions examined had a semicircular appearance, this indicated that corrosion of steel is controlled by a charge transfer process. The charge transfer resistance increased and double layer capacitance C_{dl} decreased as the concentration of inhibitor increased which indicates the adsorption of the inhibitor on the metal surface. This decrease in C_{dl} which can result from a decrease in local dielectric constant and/or an increase in the electrical double layer suggests that the thiazolidinones function by adsorption at the metal/solution interface¹¹.

In the potentiodynamic polarization measurements of mild steel in 1M H_2SO_4 in the presence of Schiff bases shows that the E_{corr} values are slightly shifted to the noble direction. b_a is affected to a slightly greater extent. This proves that though the inhibitors are under mixed control they were slightly anodic in nature. In the case of thiazolidinones E_{corr} shifts in the more noble direction with the addition of inhibitors. As concentration increases, both anodic and cathodic curves exhibit Tafel type behaviour. Though both the Tafel constants b_a and b_c were affected, b_a was displaced to a greater extent confirming the anodic nature of inhibitors.

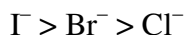
Atomic absorption spectrophotometric studies

Percentage inhibition efficiency of the inhibitors (TOAP, TMAP, TPAP) were also determined by AAS by determining the amount of iron dissolved in the corrodent solution after weight loss experiments (Table 8). The percentage inhibition efficiency obtained by this technique was found to be in good agreement with that obtained from the conventional weight loss method.

Synergism

The synergistic effect provided by the addition of halide ions I^- , Br^- and Cl^- to the solution containing 1M H_2SO_4 and the isomeric thiazolidinones were studied by

weight loss method and the data are presented in table 9. Analysis of the data revealed that the synergistic influence of halide ions follows the order.



Γ^- has highest synergistic influence among the halide ions¹². This may be explained as follows: The steel surface is originally positively charged in 1M H_2SO_4 . When Γ^- ions are added to the inhibiting solution they are strongly chemisorbed by forming chemical bonds leading to the formation of iron iodide. This strong chemisorption of Γ^- ions shifts ϕ_n (PZC) of the metal to more positive potential than in the case of Cl^- and Br^- and renders the surface more highly negatively charged. On the highly negatively charged metal surface, the protonated cationic inhibitor molecules are physisorbed due to electrostatic interaction. This interaction is higher for Γ^- than for Cl^- or Br^- due to higher magnitude of negative charge on the metal surface.

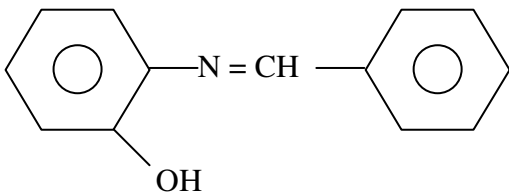
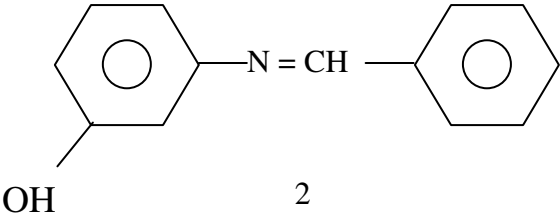
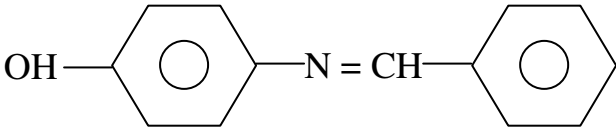
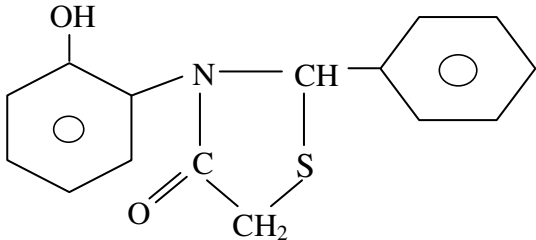
Conclusions

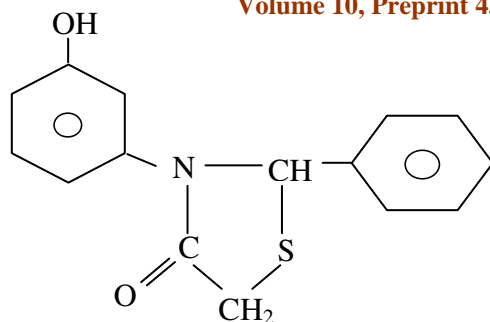
1. The three Schiff bases (OBAP, MBAP, PBAP) and their cyclisation product (TOAP, TMAP, TPAP) are effective inhibitors for corrosion of mild steel in 1M H_2SO_4 .
2. The inhibition efficiency increased with increase in inhibitor concentration and decreased with increase in temperature.
3. Cyclization does not play a significant role in enhancing the inhibition efficiency of the Schiff bases.
4. All the six inhibitors are mixed type but slightly anodic in nature.
5. The adsorption of the compounds on metal surface was found to obey Langmuir adsorption isotherm.
6. Addition of halides to the inhibitor thiazolidinone showed an increase in inhibition efficiency. The synergistic influence of halide ions follows the order $\Gamma^- > \text{Br}^- > \text{Cl}^-$.

References

1. G.Lewis,
Corros. Sci., 22 (1982) 579
2. S.Rengamani, T.Vasudevan and S.Venkata Krishna Iyer,
Ind. J. Technol., 31 (1993) 519.
3. G.Schmitt,
Br. Corros. J., 19 (1984) 165.
4. J.O'M. Bockris, B. Yang,
J. Electrochem. Soc., 19 (1984) 165.
5. C.Pillali, R.Narayan,
Corros. Sci., 23 (1983) 151.
6. S.Muralidharan, M.A. Quraishi and S.V.K. Iyer,
Corr. Sci., 37, 11 (1995) 1739.
7. Jerry March,
Advanced Organic Chemistry, Wiley & Sons, Inc., New York (1985) 460.
8. N.Subramanyan, S.V.K. Iyer and V.Kapali,
Trans. SAEST, 15 (1980) 251.
9. S.Sankarapandian, M. Anbu Kulandainathan, M. Ganesan and S.V.K. Iyer,
Bull. Electrochem., 6 (1990) 484.
10. M.S.Abdel –AAL, M.S.Morad,
Br. Corr. J. 36(4) (2001) 253.
11. E. McLafferty, N. Hackerman,
J. Electrochem. Soc., 119 (1972) 146.
12. R.Saratha, C.Marikkannu and Sivakamasundari,
Bull. Electrochem., 18(13) (2002) 141.

Table 1

Structure of the Compounds
 <p style="text-align: center;">1 OBAP Ortho benzylidene aminophenol</p>
 <p style="text-align: center;">2 MBAP Meta benzylidene aminophenol</p>
 <p style="text-align: center;">3 PBAP Para benzylidene aminophenol</p>
 <p style="text-align: center;">4 TOAP Thiazolidinone of ortho amino phenol [2-phenyl-3(2'-hydroxyphenyl) thiazolidine-4-ones]</p>

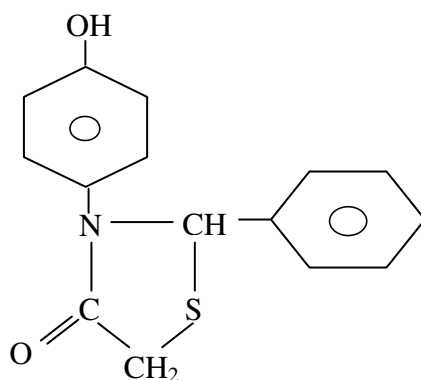


5

TMAP

Thiazolidinone of meta amino phenol

[2-phenyl-3(3'-hydroxyphenyl) thiazolidine-4-ones]



6

TPAP

Thiazolidinone of para amino phenol

[2-phenyl-3(4'-hydroxyphenyl) thiazolidine-4-ones]

Inhibition efficiencies of various concentrations of inhibitors for the corrosion of mild steel in 1M H₂SO₄ obtained by weight loss measurements at 30±1°C

Name of the inhibitor	Inhibitor Concentration (mM)	Weight loss (gms)	Inhibition Efficiency (%)	Corrosion rate (mpy)	Degree of coverage (θ)
OBAP	Blank	0.6710	-	10242.5	-
	0.5	0.0741	88.05	1131.1	0.8805
	2.5	0.0322	95.20	491.5	0.9520
	5.0	0.0136	97.97	207.5	0.9797
	7.5	0.0079	98.82	120.5	0.9882
	10.0	0.0053	99.21	80.9	0.9921
MBAP	0.5	0.3820	43.07	5831.0	0.4307
	2.5	0.1492	77.76	2277.4	0.7776
	5.0	0.0835	87.55	1274.5	0.8755
	7.5	0.0569	91.52	868.5	0.9152
	10.0	0.0470	92.89	717.4	0.9289
PBAP	0.5	0.1971	70.62	3008.6	0.7062
	2.5	0.1954	70.87	2982.6	0.7087
	5.0	0.1850	72.42	2823.9	0.7242
	7.5	0.1708	74.54	2607.7	0.7454
	10.0	0.1454	78.33	2219.4	0.7833
TOAP	0.5	0.0216	96.78	329.7	0.9678
	2.5	0.0081	98.79	123.6	0.9879
	5.0	0.0068	98.98	103.7	0.9898
	7.5	0.0056	99.16	85.4	0.9916
	10.0	0.0047	99.29	71.7	0.9929
TMAP	0.5	0.0571	91.49	871.6	0.9149
	2.5	0.0336	94.99	512.8	0.9499
	5.0	0.0327	95.12	499.1	0.9512
	7.5	0.0292	95.64	445.7	0.9564
	10.0	0.0259	96.14	395.3	0.9614
TPAP	0.5	0.0261	96.11	398.4	0.9611
	2.5	0.0087	98.70	132.8	0.9870
	5.0	0.0055	99.18	83.9	0.9918
	7.5	0.0050	99.25	76.3	0.9925
	10.0	0.0046	99.31	70.2	0.9931

Inhibition efficiencies at 10mM concentrations of inhibitor for corrosion of mild steel in 1M H₂SO₄ obtained by weight loss measurements at higher temperatures

S.No	Name of the inhibitor	Inhibition efficiency (%) at			
		303 K	313 K	323 K	333 K
1.	OBAP	99.23	98.97	95.85	93.45
2.	MBAP	93.02	91.77	90.71	85.94
3.	PBAP	78.33	77.74	67.50	61.28
4.	TOAP	99.29	95.68	95.00	93.18
5.	TMAP	96.03	95.06	94.33	93.44
6.	TPAP	99.31	98.84	98.53	97.15

Table-4

Activation energies (E_a) and free energy of adsorption (ΔG°_{ads}) for the corrosion of mild steel in 1M H₂SO₄ at selected concentrations of the inhibitors

S.No	Name of the inhibitor	E _a (kJ)	ΔG° _{ads} at various temperatures (kJ)			
			303 K	313 K	323 K	333 K
1.	Blank	25.65	-	-	-	-
2.	OBAP	75.05	-16.55	-16.33	-13.02	-12.09
3.	MBAP	50.73	-7.54	-7.64	-6.46	-5.86
4.	PBAP	63.75	-10.83	-10.73	-10.72	-9.75
5.	TOAP	71.99	-16.763	-12.515	-12.509	-11.983
6.	TMAP	58.91	-12.333	-12.149	-12.146	-12.098
7.	TPAP	59.83	-16.835	-16.027	-15.894	-14.514

Table 5

Inhibition efficiencies for the selected concentrations of the inhibitors for the corrosion of mild steel in 1M H₂SO₄ obtained by gasometric measurements

S.No	Name of the inhibitor	Inhibitor concentration(mM)	Volume of gas (cc)	Inhibition efficiency (%)
1.	OBAP	Blank	27.0	-
		0.5	3.1	88.51
		5.0	0.8	97.03
		10.0	0.3	98.88
2.	MBAP	0.5	5.2	80.74
		5.0	3.3	87.77
		10.0	2.1	92.22
3.	PBAP	0.5	8.7	67.77
		5.0	7.9	70.74
		10.0	6.1	77.40
4.	TOAP	0.5	0.9	96.66
		5.0	0.4	98.51
		10.0	0.2	99.25
5.	TMAP	0.5	2.4	91.11
		5.0	1.5	94.44
		10.0	1.2	95.55
6.	TPAP	0.5	1.1	95.92
		5.0	0.3	98.88
		10.0	0.2	99.25

Table 6

**AC-impedance parameters for mild steel for selected concentrations of the
inhibitors in 1M H₂SO₄**

S.No	Name of the inhibitor	Inhibitor concentration (mM)	R _t (ohm/cm ²)	C _{dl} (μF/cm ²)	Inhibition efficiency (%)
1.	OBAP	Blank	10.80	24.16	-
		0.5	75.88	16.62	85.76
		5.0	189.43	14.79	94.29
		10.0	211.32	12.04	94.88
2.	MBAP	0.5	82.51	15.62	86.91
		5.0	94.00	11.33	88.51
		10.0	154.96	5.22	93.03
3.	PBAP	0.5	79.01	19.45	86.33
		5.0	87.30	16.99	87.62
4.	TOAP	10.0	95.42	9.86	88.68
		0.5	80.25	18.66	86.54
		5.0	134.50	16.25	91.97
		10.0	194.70	14.02	94.45
5.	TMAP	0.5	82.42	20.53	86.89
		5.0	101.08	16.67	89.31
		10.0	106.43	10.16	89.85
6.	TPAP	0.5	127.12	17.77	91.50
		5.0	237.64	15.72	95.45
		10.0	341.49	14.25	96.83

Table 7

Corrosion parameters for mild steel with selected concentrations of the inhibitors in 1M H₂SO₄ by potentiodynamic polarization method

S.No	Name of the inhibitor	Inhibitor concentration (mM)	Tafel slopes (mV/decade)		E _{corr} (mV)	I _{corr} (μA/cm ²)	Inhibition efficiency (%)
			b _a	b _c			
1.	OBAP	Blank	113.30	149.11	-442.53	16.3	-
		0.5	75.52	144.37	-458.63	2.82	82.82
		5.0	66.75	119.27	-465.79	1.07	93.43
		10.0	67.37	113.19	-465.81	0.84	94.82
2.	MBAP	0.5	72.83	149.76	-450.51	2.22	86.38
		5.0	75.47	126.16	-466.89	1.98	87.85
		10.0	64.28	122.08	-465.95	0.97	94.04
3.	PBAP	0.5	87.57	156.09	-457.99	2.95	81.90
		5.0	102.22	153.82	-457.39	2.93	82.02
		10.0	84.88	150.26	-467.35	2.17	86.68
4.	TOAP	0.5	83.88	123.31	-478.55	2.30	85.88
		5.0	89.36	115.84	-494.37	1.60	90.18
		10.0	94.28	117.67	-498.74	0.92	94.35
5	TMAP	0.5	69.80	147.18	-478.44	1.55	90.49
		5.0	65.59	124.71	-501.83	1.48	90.92
		10.0	76.36	127.23	-509.77	0.91	94.41
6.	TPAP	0.5	64.87	125.74	-465.24	0.90	94.47
		5.0	74.51	103.65	-469.34	0.87	94.66
		10.0	66.51	101.93	-463.09	0.51	96.87

Table-8

ATOMIC ABSORPTION SPECTROSCOPY

Amount of dissolved iron present in the corrosive solution with and without inhibitors in 1M H₂SO₄

Immersion time: 3 hours

Name of the inhibitor	Inhibitor concentration (mM)	Amount of iron content (mg/l)	Inhibition efficiency (%)
TOAP	Blank	2792.8	-
	0.5	110.6	96.03
	5.0	44.96	98.39
TMAP	0.5	329.9	88.18
	10.0	154.5	94.46
TPAP	0.5	199.7	92.84
	10.0	57.40	97.94

Table-9

Synergistic effect of 1mM KCl / 1mM KBr/ 1mM KI on the inhibition efficiency of TOAP, TMAP and TPAP by weight loss method at 30±1°C

S.No	Name of the inhibitor	Inhibitor concentration (mM)	Inhibition efficiency (%)			
			Without KCl, KBr & KI	With 1mM KCl	With 1mM KBr	With 1mM KI
1.	TOAP	0.25	87.96	88.52	89.6	90.32
		0.5	88.30	89.3	90.2	91.65
		0.75	88.78	90.4	91.6	92.00
		1.0	91.56	90.9	91.4	92.3
		1.5	92.99	93.2	93.6	94.5
2.	TMAP	0.25	80.88	86.05	89.26	92.5
		0.5	81.56	86.44	89.5	93.26
		0.75	85.76	87.00	90.32	94.4
		1.0	87.93	90.22	91.6	95.2
		1.5	92.00	93.26	94.3	95.9
3.	TPAP	0.25	79.19	85.6	89.3	90.9
		0.5	80.58	89.92	90.4	91.26
		0.75	81.15	87.99	91.33	94.62
		1.0	87.68	90.35	92.65	95.00
		1.5	89.91	93.26	94.99	98.32

Figure-1

**Variation of inhibition efficiency with the concentration of the isomeric
thiazolidinones at $30\pm 1^\circ\text{C}$**

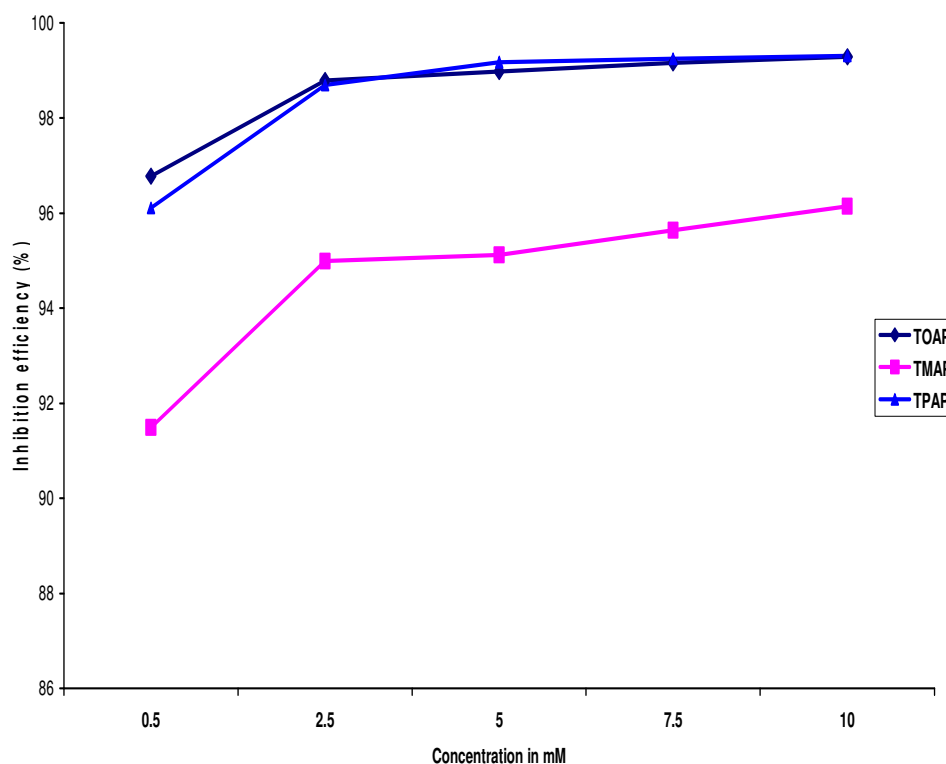


Figure-2
Langumuir's plot of thiazolidinones in 1M H₂SO₄

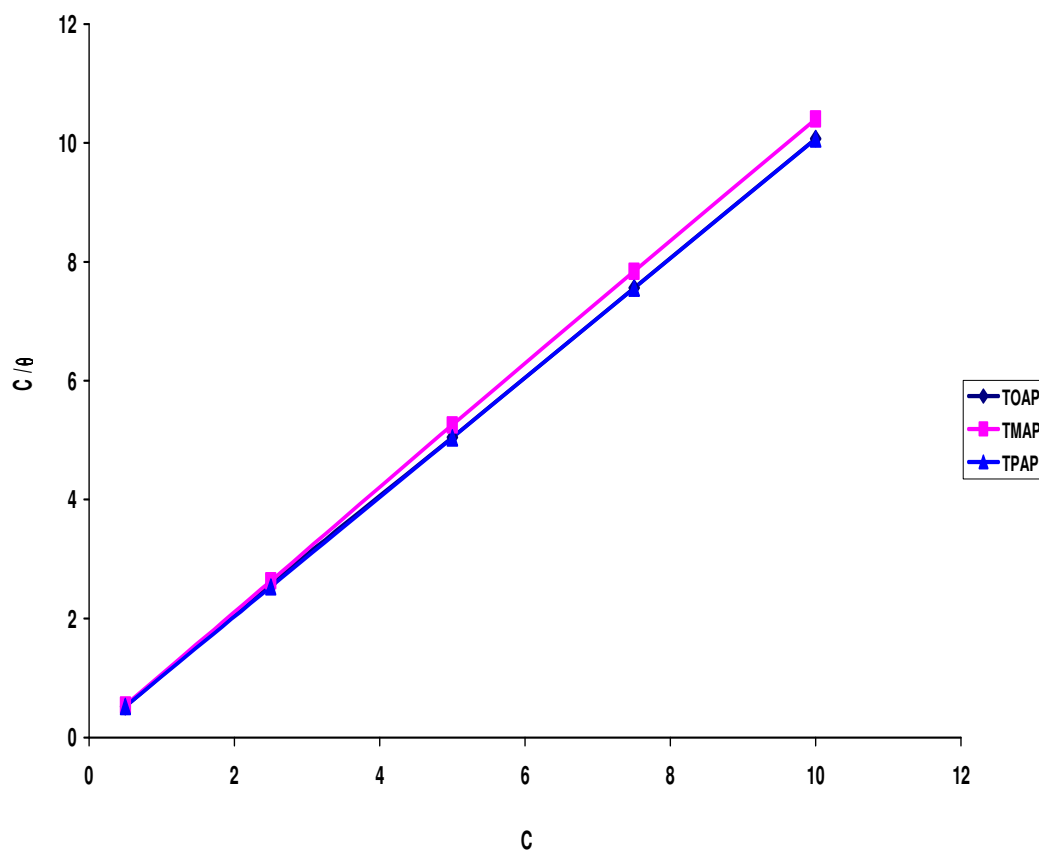


Figure-3
**Arrhenius plot of corrosion rate of mild steel in 1M H₂SO₄ solution in the
absence and presence of inhibitors**

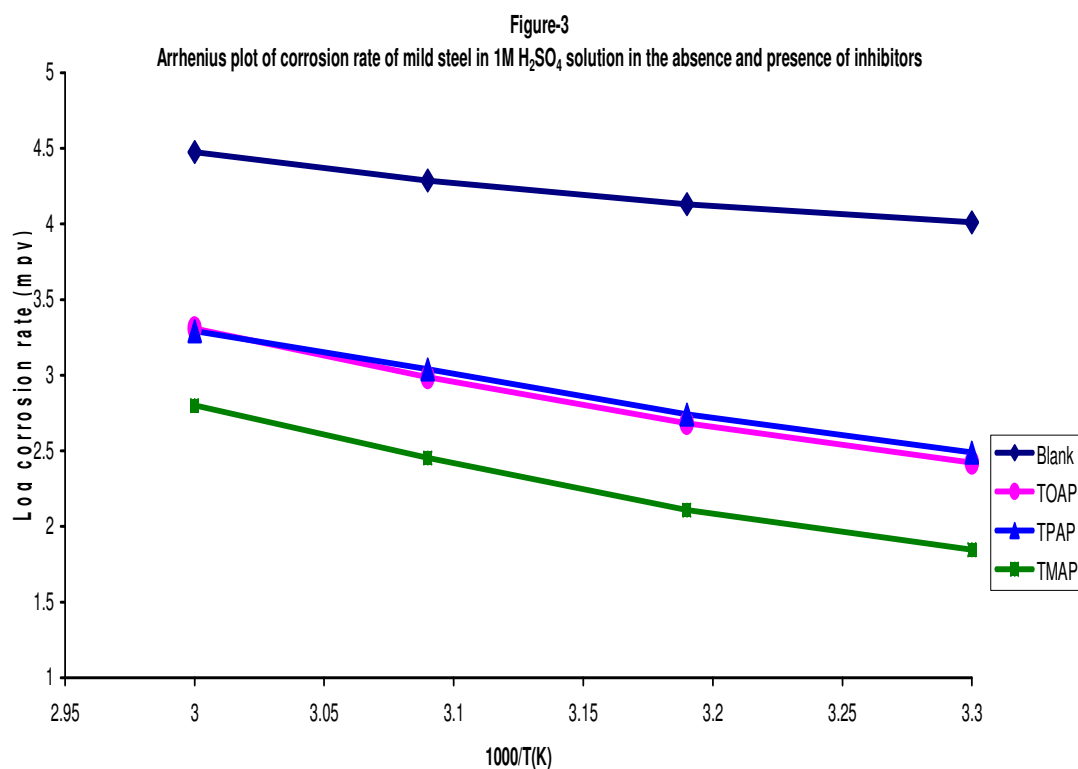


Figure-4

**Nyquist diagram for mild steel in 1M H₂SO₄ for selected
Concentrations of the inhibitor (TPAP)**

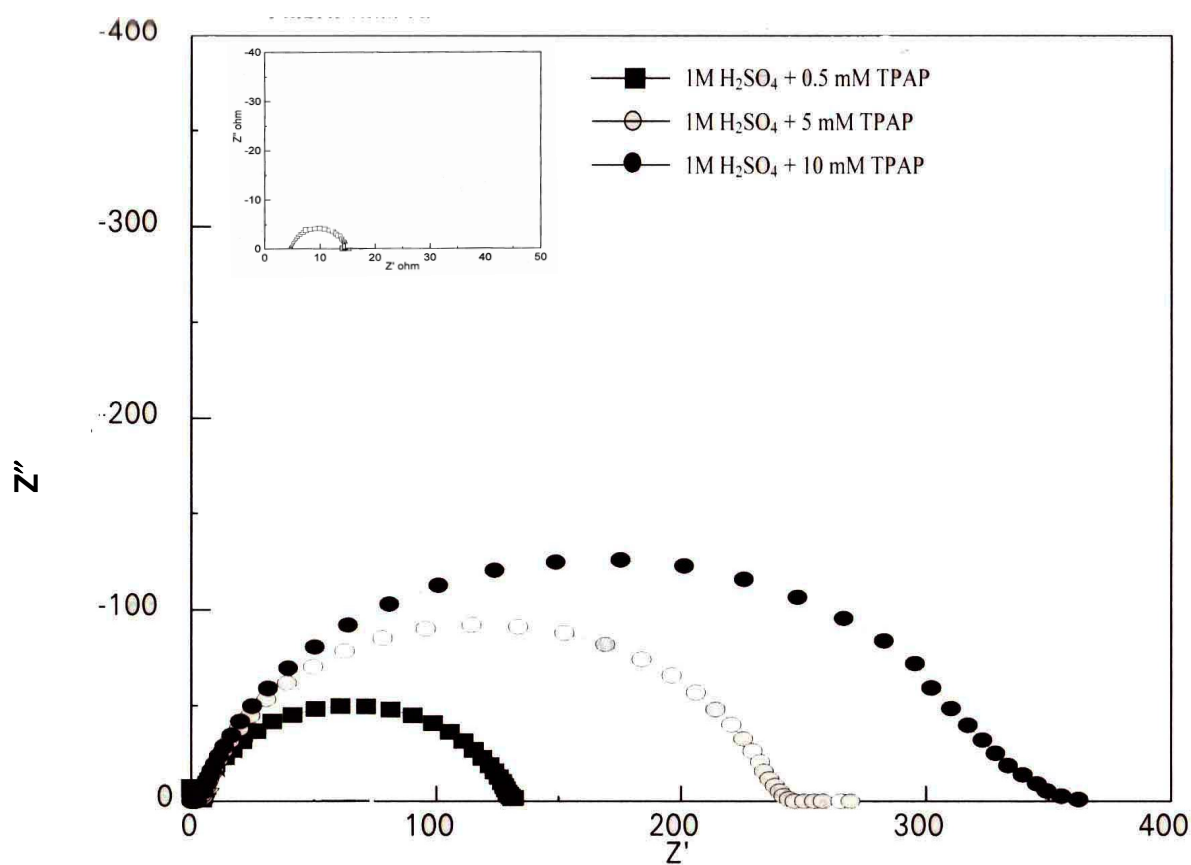


Figure-5
**Polarization curves for mild steel recorded in 1M H₂SO₄ for
selected concentrations of inhibitor (TPAP)**

